Journal of General Virology (2002), **83**, 273–281. Printed in Great Britain

A transgenic mouse model for non-immune hydrops fetalis induced by the NS1 gene of human parvovirus B19

Hiroshi Chisaka,[1,2] Eiji Morita,[1] Kazuko Murata,[1,3] Naoto Ishii,[1] Nobuo Yaegashi,[2] Kunihiro Okamura[2] and Kazuo Sugamura[1]

[1,2] Department of Microbiology and Immunology[1] and Department of Obstetrics and Gynecology[2], Tohoku University Graduate School of Medicine, 2-1 Seiryo-machi, Aoba-ku, Sendai 980-8575, Japan

[3] CREST Program of the Japan Science and Technology Corporation, Sendai 980-8575, Japan

Human parvovirus B19 (B19) infection during pregnancy is associated with the adverse foetal outcome known as non-immune hydrops fetalis (NIHF). Although B19 is known to infect erythroid-lineage cells *in vivo* as well as *in vitro*, the mechanism leading to the occurrence of NIHF is not clear. To investigate the possible involvement of the B19 non-structural protein NS1 in NIHF, three independent lines of transgenic mice were generated that expressed NS1 under the control of the Cre-*loxP* system and the GATA1 promoter. Two of the three lines expressed NS1 in erythroid-lineage cells. Most of the transgenic mice died at the embryonic stage, some of which developed hydropic changes caused by severe anaemia at embryonic day 15·5 (E15·5). Histological examination of embryos at E15·5 showed significantly fewer erythropoietic islands in the liver parenchyma, whereas their hearts showed no abnormal signs, such as cardiomegaly and apoptotic cells. The NS1-transgenic mouse lines established here provide an animal model for human NIHF and suggest that NS1 plays a crucial role in the adverse outcome associated with intrauterine B19 infection in humans.

Introduction

Human parvovirus B19 (B19) was discovered in the sera of healthy blood donors (Cossart *et al.*, 1975) and was defined to be the causative agent of erythema infectiosum (fifth disease) in children (Anderson *et al.*, 1983) and polyarthropathy syndrome in adults (Brown & Young, 1997). B19 is a small, single-stranded DNA virus and is characterized by its target specificity for human erythroid-lineage cells, which is due in part to the distribution of its receptor, the P antigen (Brown *et al.*, 1993, 1994). B19 infection causes human aplastic conditions, such as chronic anaemia in immunocompromised hosts, transient aplastic crisis and probably some cases of non-immune hydrops fetalis (NIHF) (Brown *et al.*, 1984; Yaegashi *et al.*, 1999; Young, 1988). The anaemia induced by B19 infection is of minor clinical significance in healthy children and adults; however, it becomes critical in those afflicted with haemolytic diseases, such as sickle cell anaemia, hereditary spherocytosis and thalassaemia (Kelleher *et al.*, 1983; Levy *et al.*, 1997). The pathogenesis of aplastic crisis in patients with haemolytic disease is accounted for by the short life-span of red blood cells. The turnover of erythroid-lineage cells is rapid in these patients and B19 infection induces the acceleration of death of erythroid-lineage cells, resulting in severe anaemia (Kelleher *et al.*, 1983; Levy *et al.*, 1997). Similarly, foetuses are thought to be severely affected, particularly during the early hepatic stage of haematopoiesis, as the half-life of red blood cells is apparently shorter in this haematopoietic stage compared with the later bone marrow/splenic haematopoietic stage (Yaegashi *et al.*, 1989, 1998). The risk of an adverse foetal outcome is approximately 10% when mothers are infected with B19, and increases if maternal infection occurs during the first 20 weeks of gestation (Miller *et al.*, 1998; Yaegashi *et al.*, 1998). Epidemiological studies have also shown that intrauterine B19 infection is causatively related to NIHF and intrauterine foetal death without malformations (Brown *et al.*, 1984; Miller *et al.*, 1998; Yaegashi *et al.*, 1994). However, the mechanism of induction of NIHF by B19 infection, the cause of the severe anaemia, has not yet been clarified.

B19 carries three major viral proteins: VP1 and VP2, virus capsid proteins, and NS1, a non-structural protein (Ozawa *et*

Author for correspondence: Kazuo Sugamura.
Fax +81 22 717 8097. e-mail sugamura@mail.cc.tohoku.ac.jp

al., 1987). NS1 is known to be implicated in virus replication (Ozawa *et al*., 1986), activation of virus and cellular gene transcription (Doerig *et al*., 1990; Moffatt *et al*., 1996; Sol *et al*., 1993) and target-cell cytotoxicity (Moffatt *et al*., 1998; Momoeda *et al*., 1994; Ozawa *et al*., 1988). We showed previously that NS1-induced cytotoxicity was mediated by caspase 3 and inhibited by the overexpression of Bcl-2, suggesting that NS1 is an apoptotic protein of B19 (Moffatt *et al*., 1998). In addition, the commitment of B19-infected cells to undergo apoptosis is combined with their accumulation in the G_2/M phase of the cell cycle (Sol *et al*., 1999). Based on these observations, we speculated that the severe anaemia of the B19-infected foetus might result from the expression of cytotoxic NS1 in erythroid precursor cells. However, there has been no direct evidence that expression of NS1 induces NIHF *in vivo*. Hence, to establish a mouse model of human NIHF, we generated NS1-transgenic mice in which NS1 expression was strictly confined to erythroid-lineage cells.

Methods

■ **Plasmid construction.** An expression plasmid for NS1, pIE3.9int-NS1, was constructed as follows: an *NS1* gene fragment (2·1 kb) was derived from pOPRSV-NS1 (Moffatt *et al*., 1996), digested with *Not*I and inserted into the *Not*I site of pIE3.9int-polyA (Onodera *et al*., 1997). Another expression plasmid for NS1, pIE3.9int-loxP-neo-loxP-NS1, was constructed as follows: the 2·1-kb *NS1* gene was inserted into the *Not*I site of ploxP-neo and a 3·9-kb DNA fragment derived from the resultant plasmid, ploxP-neo-loxP-NS1, was inserted into the *Not*I site of pIE3.9int-polyA. A Cre-expression plasmid, pIE3.9int-cre, was constructed as follows: the bacteriophage P1 *cre* gene (1·1 kb) derived from pBS185 (Gibco-BRL) was inserted into the *Not*I site of pIE3.9int-polyA. All plasmid DNA constructs were confirmed by sequencing (Fig. 1A).

■ **Generation of transgenic mouse lines.** After removing the vector DNA fragments, the individual constructs of *IE3.9int-loxP-neo-loxP-NS1* and *IE3.9int-cre* were purified and microinjected into fertilized eggs of BDF1 mice, which were then implanted into foster mothers. The resulting progeny were screened for integration of the transgenes by Southern blot analysis and PCR using mouse tail DNA and maintained by mating with BDF1 mice. We thus established a GATA1-Cre transgenic mouse line (line 453) with the *IE3.9int-cre* gene and three independent GATA1-Neo-NS1 transgenic mouse lines (lines 464, 468 and 175) with the *IE3.9int-loxP-neo-loxP-NS1* gene. Heterozygosity was determined by examining more than ten pups from breeding with non-transgenic BDF1 mice for their genotypes by PCR analysis (see below). CAG-CAT-Z transgenic mice (Sakai & Miyazaki, 1997) were maintained by mating with BDF1 mice. The CAG-CAT-Z construct consists of the CAG promoter (*CAGGS*, cytomegalovirus immediate-early enhancer–chicken β-actin hybrid promoter), *loxP-CAT-loxP* and the *lacZ* gene and was used to confirm that the Cre/*loxP* site-specific recombination system was functional in the F1 progeny that resulted from a cross between CAG-CAT-Z transgenic mice and GATA1-Cre transgenic mice.

■ **Cell culture.** K562 is an erythroleukaemia cell line, UT-7/Epo is a megakaryocytic cell line adapted for growth dependent on erythropoietin (Shimomura *et al*., 1992), COS7 is a simian virus 40-transformed fibroblast cell line and MT-1 is a human adult T-cell leukaemia cell line. The cell lines were maintained in RPMI 1640 medium containing 10% FCS and 2 U erythropoietin (Kirin Brewery Pharm. Res. Lab.) was added to the medium for the UT-7/Epo cells.

■ **Immunoprecipitation and immunoblotting.** Immunoprecipitation and immunoblotting were performed as described previously (Moffatt *et al*., 1996, 1998). In brief, cells were lysed in RIPA buffer (pH 7·5) containing 10 mM Tris–HCl (pH 7·5), 1% NP-40, 0·1% sodium deoxycholate, 0·1% SDS, 150 mM NaCl, 1 mM EDTA and 10 μg/ml aprotinin. The lysates were then immunoprecipitated with a mAb specific for NS1 coupled to protein A–Sepharose beads and anti-mouse IgG (Zymed). The immunoprecipitates were separated on a 10% polyacrylamide gel and transferred to PVDF filters (Millipore). After being incubated in PBS containing 3% BSA, the blots were probed with a mAb against NS1 protein and immune complexes were visualized by enhanced chemiluminescence according to the manufacturer's instructions (Amersham).

■ **Southern blot analysis.** Tissue DNA was isolated from tails of mice using the QIAamp Tissue kit (Qiagen). An aliquot (10 μg) of the DNA was digested with *Xba*I, separated on a 1·0% agarose gel and transferred onto Gene Screen Plus (NEN Research Products) and then hybridized overnight at 42 °C in 6 × SSC/0·5% SDS using ^{32}P-labelled probes corresponding to the NS1 coding region (398 bp) or the Cre coding region (328 bp). The membrane was washed in 2 × SSC/0·1% SDS and exposed to X-ray film. The signal was quantified with an image analyser (BAS2000, Fuji) and the copy number was estimated by using the control plasmid to generate the transgene.

■ **PCR analysis to genotype the transgenic mice.** Mouse tails and embryos were lysed with 0·5% NP-40, 1 μg/μl proteinase K and *Taq* TM PCR buffer (Takara Shuzo) for 2 h and incubated at 95 °C. Approximately 1 μg of DNA extracted from the lysates was subjected to 35 cycles of amplification on a thermal cycler. The primers used for amplification of sequences within the *NS1* gene were N1 (5′ CACAGACACCAGTATCAGCAGCAGT 3′) and N2 (5′ CACACATAATCAACCCCAACTAACG 3′), which produced 261-bp DNA fragments. The primers used for amplification of sequences within the *cre* gene were C1 (5′ AAAAACTATCCAGCAACATT 3′) and C2 (5′ TAACATTCTCCCACCGTCAG 3′), which produced 328-bp DNA fragments. The primers used for amplification of sequences within the *lacZ* gene were L1 (5′ GCGTTACCCAACTTAATCG 3′) and L2 (5′ TGTGAGCGAGTAACAACC 3′), which produced 320-bp DNA fragments (Sakai & Miyazaki, 1997). PCR products were analysed by electrophoresis in 2% agarose gels.

■ **Detection of β-galactosidase in whole embryos.** For whole-mount X-Gal staining, embryos were removed at embryonic day 10·5 (E10·5). They were fixed at 4 °C for 2 h in 1% formaldehyde, 0·2% glutaraldehyde and 0·02% NP-40 in PBS. After washing with PBS, they were incubated at 37 °C for 5 h in 5 mM $K_3Fe(CN)_6$, 5 mM $K_4Fe(CN)_6$, 2 mM $MgCl_2$ and 1 mg/ml X-Gal in PBS.

■ **Blood analysis.** Embryonic blood was obtained from umbilical cord vessels using microhematocrit tubes (Microcaps, Drummond Scientific). Haematocrit measurements of embryonic blood were taken after centrifugation for 3 min. Giemsa staining of blood smears was performed as described previously (Socolovsky *et al*., 1999).

■ **RNA isolation and RT–PCR analysis.** To confirm expression of the *NS1* gene mRNA, we performed RT–PCR. Total RNA was isolated from liver and spleen with Trizol reagent (Technologies TM) according to the manufacturer's instructions. The RNA concentration was determined from the absorbance. The isolated RNA was reverse-transcribed to cDNA using random hexamers as primers and Superscript II reverse transcriptase (Life Technologies) according to the manufacturer's in-

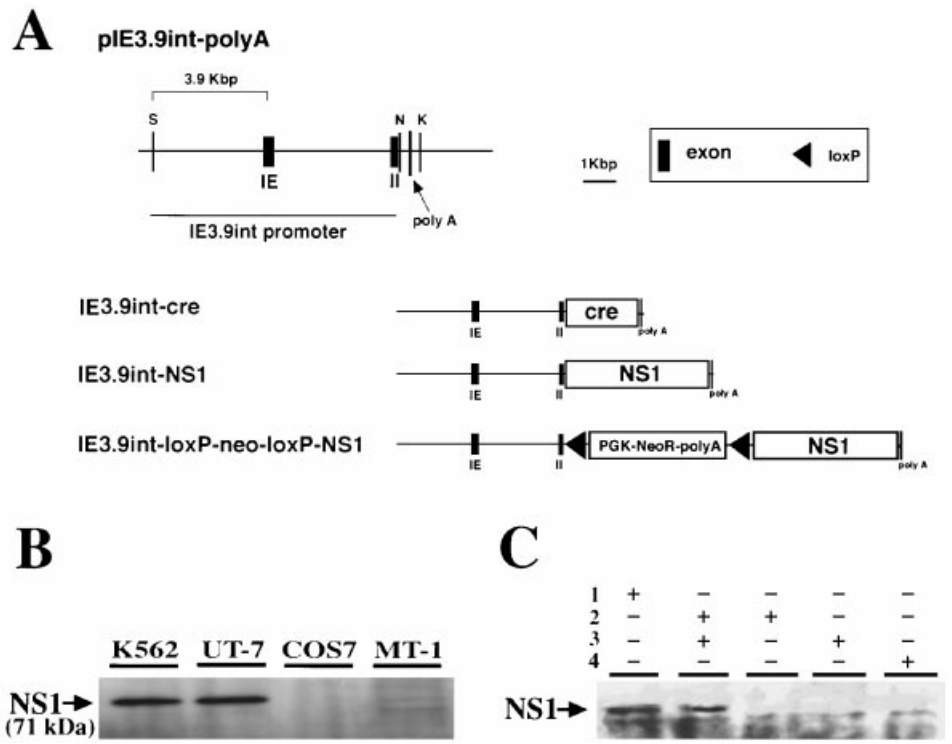

Fig. 1. Schematic diagrams of DNA constructs and their Cre-mediated recombination. (A) DNA constructs used in the Cre/*loxP* site-specific recombination system. See Methods for details of plasmid construction. We used the *loxP-neo-loxP* DNA construct to hamper the expression of NS1 in the absence of Cre-mediated recombination. IE indicates the relative position of the erythroid first exon. Abbreviations for restriction enzyme sites: S, *Sal*I; N, *Not*I; K, *Kpn*I. (B) pIE3.9int-NS1 was transiently transfected into the erythroid cell lines K562 and UT-7 and the non-erythroid cell lines COS7 and MT-1. Cells were then analysed for NS1 expression by Western blotting with an anti-NS1 mAb. The arrow indicates the position of NS1. (C) Cre-mediated recombination *in vitro*. K562 cells were transiently transfected with pIE3.9int-NS1 (1), pIE3.9int-loxP-neo-loxP-NS1 (2), pIE3.9int-cre (3) and/or pIE3.9int-polyA (4) as shown above the lanes. They were then analysed for NS1 expression by Western blotting. The arrow indicates the position of NS1.

structions and the cDNA was then used as a template for PCR. PCR was performed under the same conditions as the genotype analysis.

■ **Real-time RT–PCR.** Real-time RT–PCR was performed as described previously (Barbany *et al.*, 2000; Bièche *et al.*, 1999). cDNA was synthesized from 3 μg total RNA extracted from each embryonic liver and then subjected to PCR amplification. The PCR was performed in a 50 μl volume. The PCR mixture contained 2 μl of each appropriate RT reaction cDNA sample, 5 μl 10 × SYBR Green PCR buffer, 5 μl 25 mM $MgCl_2$, 4 μl dNTP mix, 0·5 μl AmpErase UNG, 15 pmol forward and reverse primer and 0·25 μl AmpliTaq Gold DNA polymerase (Perkin-Elmer Applied Biosystems). All PCRs and detection of real-time fluorescent energy were performed using an ABI Prism 7700 Sequence Detection system (Perkin-Elmer Applied Biosystems). The thermal cycling conditions consisted of an initial denaturation step at 95 °C for 10 min and 50 cycles at 95 °C for 15 s and 60 °C for 1 min. Each PCR result was calculated from a standard curve, constructed by using various concentrations of *NS1* cDNA (10-fold serially diluted cDNA ranging between 10^{-10} and 10^{-14} g). A strong linear relationship between the threshold cycle (Ct) and the log of the starting cDNA copy number was continually demonstrated ($r^2 > 0{\cdot}98$; data not shown). The β-actin signal was used to normalize the amount of input cDNA. Experiments were performed with duplicates for each data point.

■ **Whole-mount *in situ* hybridization.** Embryos were fixed in 4% paraformaldehyde on ice for several hours and processed for whole-mount *in situ* hybridization. After dehydration and rehydration, the embryos were incubated with digoxigenin-labelled probe and stained with the alkaline phosphate substrate, NBT/BCIP, under the conditions recommended by the manufacturer (Boehringer Mannheim). Antisense and sense RNAs of NS1 were labelled with digoxigenin–UTP and used as probes.

Results

The Cre/*loxP* recombination system induces conditional expression of NS1 in erythroid-lineage cells

The NS1 protein of human parvovirus B19 is known to be cytotoxic, due to its apoptosis-inducing activity in various types of cell (Moffatt *et al.*, 1998; Morey *et al.*, 1993; Sol *et al.*, 1999). Thus, establishing transgenic mice that expressed the NS1 protein continuously presented special challenges. We first constructed a plasmid, pIE3.9int-NS1, that consisted of the *NS1* gene driven by the IE3.9int promoter of the *GATA*-1 gene (Fig. 1A; Onodera *et al.*, 1997). Transfection of pIE3.9int-NS1 induced the expression of the NS1 protein in the erythroid cell lines K562 and UT-7, but not in lines derived from other

Table 1. Genotypes of F1 progeny of three GATA1-Neo-NS1-transgenic mice, each crossed with a GATA1-Cre-transgenic mouse

F1 progeny were genotyped at various embryonic and neonatal stages by PCR, as described in Methods.

Embryonic age	loxP-NS$^+$/cre$^+$ (%)	loxP-NS$^+$/cre$^-$	loxP-NS$^-$/cre$^+$	loxP-NS$^-$/cre$^-$	Total
Line 468					
At weaning	30 (15)	59	47	59	195
E9·5	6 (27)	4	8	4	22
E10·5	6 (25)	4	6	8	24
E11·5	12 (27)	10	12	10	44
E12·5	20 (31)	14	12	18	64
E13·5	13 (20)	15	19	18	65
E14·5	6 (12)	16	12	16	50
E15·5	9 (15)	18	14	18	59
E16·5	5 (11)	18	12	12	47
Line 175					
At weaning	5 (5)	40	29	30	104
E12·5	4 (12)	9	7	13	33
E13·5	4 (12)	10	8	12	34
E14·5	1 (3)	9	10	7	27
Line 464					
At weaning	0	29	35	33	97
E7·5	0	10	14	6	30
E8·5	0	10	6	5	21
E9·5	0	6	10	10	27

types of cell, such as COS7 and MT-1 (Fig. 1B), suggesting that the IE3.9int promoter worked specifically in erythroid cells. By using pIE3.9int-NS1, we attempted to generate NS1-expressing transgenic mice, but were unsuccessful (data not shown). Hence, to obtain founder mice, we used the Cre/*loxP* site-specific recombination system (Lakso *et al*., 1992; Orban *et al*., 1992). We designed two plasmids for this purpose, pIE3.9int-loxP-neo-loxP-NS1, in which the *neo* gene flanked by *loxP* sites was inserted between the promoter and the *NS1* gene, and pIE3.9int-cre, which encoded the Cre recombinase (Fig. 1A). The use of these plasmids permitted the conditional expression of NS1. When plasmids pIE3.9int-loxP-neo-loxP-NS1 and pIE3.9int-cre were transfected simultaneously into K562 cells, the cells expressed the NS1 protein, whereas transfection of plasmid pIE3.9int-loxP-neo-loxP-NS1 alone did not induce NS1 expression (Fig. 1C). These results indicate that the *NS1* gene recombined directly with the IE3.9int promoter after Cre-mediated excision of the *neo* gene from pIE3.9int-loxP-neo-loxP-NS1 and that the recombined DNA construct drove the successful expression of the *NS1* gene.

Establishment of transgenic mouse lines

We first established a GATA1-Cre transgenic mouse line (line 453) expressing *IE3.9int-cre*. In order to confirm that the Cre recombinase in GATA1-Cre mice was functional, we used transgenic mice bearing a reporter gene construct, *CAG-CAT-Z*, which directs the expression of the *E. coli lacZ* gene upon the Cre-mediated excision of the *CAT* gene located between the CAG promoter and the *lacZ* gene (Sakai & Miyazaki, 1997). GATA1-Cre mice were crossed with heterozygous CAG-CAT-Z mice. The yolk sacs of the F1 progeny mice were examined at E10 for LacZ expression by X-Gal staining, because the yolk sac is an active haematopoietic centre at E10. In the F1 progeny, positive X-Gal staining was observed in the yolk sacs derived from embryos that carried both the *CAG-CAT-Z* transgene and the *IE3.9int-cre* transgene, indicating that the Cre recombinase of the GATA1-Cre mice was functional *in vivo* (data not shown).

We next established three independent GATA1-Neo-NS1-transgenic mouse lines (lines 464, 468 and 175) containing *IE3.9int-loxP-neo-loxP-NS1* transgenes. In all three lines, the transgene was unable to drive expression of the *NS1* gene because the *neo* gene was inserted between the IE3.9int promoter and the *NS1* gene (Fig. 1A). The F1 progeny of the GATA1-Neo-NS1 lines 464, 468 and 175 respectively had 5, 30 and 70 copies of the *NS1* gene, as determined by Southern blot analysis (data not shown). We also confirmed that the founder mice carried the transgenes in a heterozygous manner and that the transgenes were transmitted to their progeny according to Mendelian expectations.

In order to obtain transgenic mice expressing NS1 in erythroid-lineage cells, we crossed heterozygous GATA1-Neo-NS1 mice with heterozygous GATA1-Cre mice; a quarter

of their progeny were expected to express the *NS1* gene due to direct recombination between the IE3.9int promoter and the *NS1* gene. The F1 progeny were genotyped and shown to include loxP-NS$^+$/cre$^+$ mice carrying both the *IE3.9int-cre* and *IE3.9int-loxP-neo-loxP-NS1* transgenes, loxP-NS$^+$/cre$^-$ mice carrying only *IE3.9int-loxP-neo-loxP-NS1*, loxP-NS$^-$/cre$^+$ mice carrying only *IE3.9int-cre* and loxP-NS$^-$/cre$^-$ wild-type mice.

NS1 expression in the haematopoietic organs of F1 progeny obtained from crossing GATA1-Neo-NS1 mice with GATA1-Cre mice

We first analysed 195 F1 progeny obtained from crossing line 468 of the heterozygous GATA1-Neo-NS1 mice with heterozygous GATA1-Cre mice at weaning. The number of loxP-NS$^+$/cre$^+$ mice was approximately half that of the loxP-NS$^+$/cre$^-$, loxP-NS$^-$/cre$^+$ or wild-type mice at weaning (Table 1). These weanlings were examined by RT–PCR for expression of the *NS1* gene in the spleen, which is a haematopoietic organ. *NS1* gene expression was detected in loxP-NS$^+$/cre$^+$ mice but not in the other genotypes (Fig. 2A). Hence, we genotyped the F1 progeny further at various days of gestation. The number of loxP-NS$^+$/cre$^+$ embryos was not significantly less before E13·5 compared with the other F1 littermates, but decreased appreciably after E13·5 (Table 1). We also examined the embryos by RT–PCR at E12·5 for expression of the *NS1* gene in the liver, which is an embryonic haematopoietic organ. Of more than ten embryos in the same uterus, *NS1* gene expression was detected in only three loxP-NS$^+$/cre$^+$ embryos (Fig. 2B) and not in the other genotypes. Furthermore, we examined the quantitative expression of the *NS1* gene in these three loxP-NS$^+$/cre$^+$ embryos by real-time RT–PCR. The cDNA copy number of the lane 3 embryo was approximately twofold higher compared with the lane 2 and lane 4 embryos (Fig. 2B). These data may suggest that the embryos lived to different stages because NS1 was expressed at different levels.

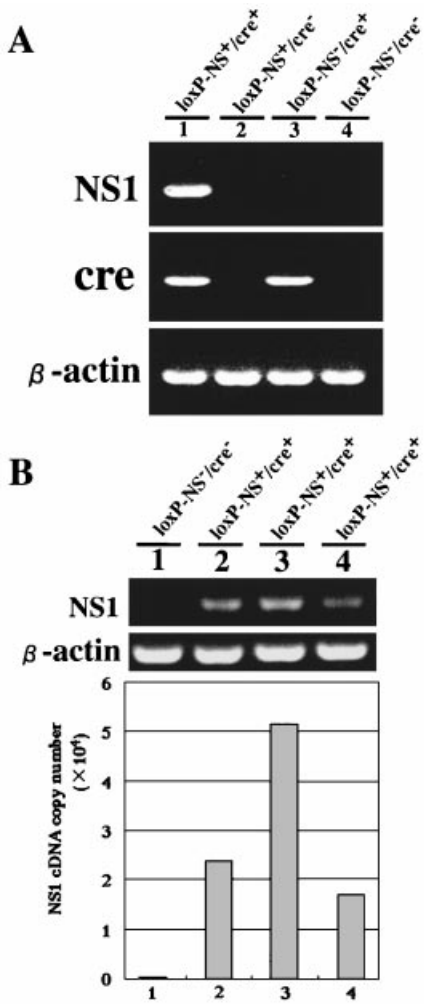

Fig. 2. RT–PCR analysis of F1 progeny obtained from GATA1-Cre × GATA1-Neo-NS1 (line 468) mice and comparison of NS1 expression in the livers of loxP-NS$^+$/cre$^+$ embryos in the same uterus. (A) Total RNA was isolated from spleens of loxP-NS$^+$/cre$^+$, loxP-NS$^+$/cre$^-$, loxP-NS$^-$/cre$^+$ and loxP-NS$^-$/cre$^-$ (wild-type) mice and subjected to RT–PCR. *NS1* mRNA was detected only in the spleen of the loxP-NS$^+$/cre$^+$ mouse (lane 1) and not in the spleens of mice of other genotypes. *cre* mRNA was detected in the spleens of loxP-NS$^+$/cre$^+$ and loxP-NS$^-$/cre$^+$ mice (lanes 1 and 3). (B) Expression of the *NS1* gene in the liver of E12·5 F1 embryos obtained from GATA1-Cre × GATA1-Neo-NS1 (line 468) mice. RT–PCR showed expression of the *NS1* gene in the livers of the three loxP-NS$^+$/cre$^+$ embryos (lanes 2–4) but not in the loxP-NS$^-$/cre$^-$ (wild-type) embryo (lane 1). The levels of *NS1* mRNA expression in embryonic livers were also measured by real-time RT–PCR analysis. The initial copy number was inferred from a standard curve performed in parallel using known amounts of *NS1* cDNA.

GATA1-driven expression of NS1 *in vivo* induces hydropic changes and death in embryos

Interestingly, we found embryos with hydropic phenotypes at E15·5, in which the skin was remarkably oedematous and pale, but the embryos were without apparent malformation (Fig. 3A). Their genotypes were confirmed to be loxP-NS$^+$/cre$^+$. Haematocrits of the umbilical cord blood were 20·8 ± 1·4% (mean ± SEM) in the loxP-NS$^+$/cre$^+$ embryos and 40·8 ± 1·7% in wild-type mice at E15·5. The haematocrits of the loxP-NS$^+$/cre$^-$ and loxP-NS$^-$/cre$^+$ embryos were similar to those of wild-type embryos (data not shown). Furthermore, umbilical cord blood of the loxP-NS$^+$/cre$^+$ embryos at E15·5 contained a much smaller proportion of erythrocytes without nuclei than that of wild-type mice (Fig. 3B), revealing a disturbance of haematopoiesis (Mucenski *et al.*, 1991; Socolovsky *et al.*, 1999) in the loxP-NS$^+$/cre$^+$ embryos. Histological examination of the foetal livers, where active haematopoiesis occurs, also demonstrated that there were significantly fewer erythropoietic islands in the liver parenchyma of loxP-NS$^+$/cre$^+$ embryos than in those of wild-type mice (Fig. 3C). We also performed a histological examination of the foetal hearts. The structure of the heart in loxP-NS$^+$/cre$^+$ embryos was normal and myocardial damage, such as apoptosis or necrosis, was not observed (data not shown). These results suggest that IE3.9int promoter-driven

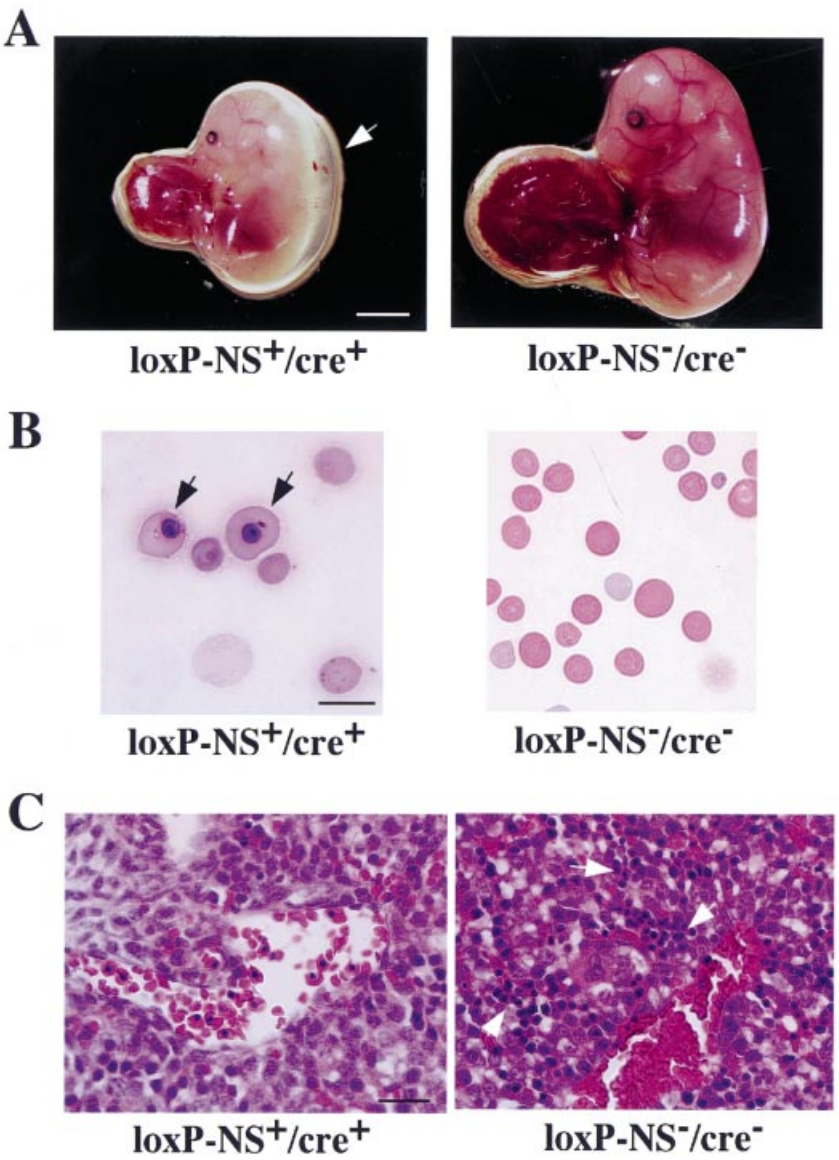

Fig. 3. Phenotypic comparison of E15·5 embryos obtained from GATA1-Cre × GATA1-Neo-NS1 (line 468) mice. (A) Phenotypes of whole embryos. The arrow indicates the hydropic skin of the embryo. Bar, 3 mm. (B) Giemsa staining of blood smears. The vast majority of cells seen in the loxP-NS^{-}/cre^{-} (wild-type) embryo were large, non-nucleated erythrocytes, whereas very few erythrocytes were seen in the loxP-NS^{+}/cre^{+} embryos and many of these had a nucleus (arrows). Bar, 15 μm. (C) Haematoxylin and eosin staining of liver tissues. Islands of haematopoietic cells were observed far less frequently in the loxP-NS^{+}/cre^{+} liver than in the wild-type liver. The sinusoids contained numerous islands of haematopoietic cells (arrows) and the vessels were filled with non-nucleated erythrocytes in the wild-type liver. Bar, 60 μm.

expression of NS1 resulted in a disruption of foetal erythropoiesis, which caused foetal death with severe anaemia.

In order to examine further the fatal effects of NS1 in mice, we crossed line 175 of heterozygous GATA1-Neo-NS1 mice with the heterozygous GATA1-Cre mice and observed the F1 progeny. At weaning, five of 104 F1 mice were loxP-NS^{+}/cre^{+}, which was fewer than when line 468 mice were used for the cross (Table 1), suggesting that NS1 expression induced more severe embryonic damage in line 175 than in line 468. We also generated F1 progeny from crossing line 464 of heterozygous GATA1-Neo-NS1 mice with GATA1-Cre mice. However, at weaning, none of the 97 progeny mice had the loxP-NS^{+}/cre^{+} genotype, suggesting that NS1 expression in these embryos resulted in prenatal lethality (Table 1). We then genotyped F1 embryos from line 464 at various days of gestation. Wild-type, loxP-NS^{+}/cre^{-} and loxP-NS^{-}/cre^{+} embryos were recovered between E7·5 and E9·5, but no loxP-NS^{+}/cre^{+} embryos were seen (Table 1). Hence, we examined expression of the *NS1* mRNA at E6·5 by whole-mount *in situ* hybridization. NS1 expression was confirmed in loxP-NS^{+}/cre^{+} embryos, but not

in wild-type embryos (data not shown). These results suggest that *NS1* gene expression at an early embryonic stage induced early embryonic lethality.

Discussion

The non-structural protein, NS1, of B19 is thought to play a critical role in the pathogenesis of diseases associated with B19 infection. Contributions to virus replication (Ozawa *et al.*, 1986), activation of virus and cellular gene transcription (Doerig *et al.*, 1990; Moffatt *et al.*, 1996; Sol *et al.*, 1993) and target cell apoptosis (Moffatt *et al.*, 1998; Momoeda *et al.*, 1994; Ozawa *et al.*, 1988) have been suggested. Since B19 can not infect mice, we established mice that expressed NS1 to analyse the mechanisms of B19 infectious disease. We suspected that it might be difficult to establish transgenic mouse lines that expressed NS1 stably, because of its apoptosis-inducing activity. Hence, we engineered mice expressing the *NS1* transgene, with expression restricted to erythropoietic cells by using the IE3.9int promoter (GATA1 promoter), which is known to be activated specifically in erythroid-lineage cells (Fujiwara *et al.*, 1996; Onodera *et al.*, 1997; Pevny *et al.*, 1991), and the Cre/*loxP* recombination system (Lakso *et al.*, 1992; Orban *et al.*, 1992). Using this approach, three GATA1-Neo-NS1-transgenic mouse lines (lines 464, 468 and 175) were generated and appeared to be suitable animal models of human intrauterine B19 infection.

In the F1 progeny from crosses between line 468 GATA1-Neo-NS1 mice and GATA1-Cre mice, approximately half the loxP-NS^+/cre^+ genotype mice, which expressed NS1, were born alive and the other half died *in utero*, presenting with hydropic features and severe anaemia, probably due to the disruption of erythropoiesis. These phenotypes of the NS1-transgenic mice are similar to those of human NIHF, which occurs when there is an intrauterine B19 infection during pregnancy, and indicate that the NS1-transgenic mice can be used as an animal model of this disease. In contrast, GATA-1-deficient mice, despite showing completely defective erythropoiesis in the primitive haematopoietic centre (Fujiwara *et al.*, 1996; Pevny *et al.*, 1991; Shivdasani & Orkin, 1996), do not show hydropic characteristics. The NS1 protein is known to have a variety of functions in addition to inducing apoptosis, as outlined above. Recently, we demonstrated B19-induced G_2 cell-cycle arrest with suppression of nuclear import of cyclin B1, which was thought to be mediated by NS1 expression (Morita *et al.*, 2001). Thus, it is possible that these various functions associated with the NS1 protein influence the occurrence of hydropic changes in the foetus.

The severity of embryonic damage in the loxP-NS^+/cre^+ F1 progeny varied with the transgenic line: loxP-NS^+/cre^+ F1 progeny resulting from crosses with line 175 mice were recovered at weaning, but in a significantly lower proportion than those resulting from line 468, and none were recovered after E7·5 from line 464, indicating that the NS1 gene induced the most severe embryonic damage in line 464. We believe that the severity of embryonic damage is primarily dependent on the level of NS1 expression in the F1 progeny, but also on the leakiness of NS1 expression during embryogenesis. Since line 464 showed the lowest *NS1* copy number of the three transgenic lines, the level of *NS1* gene expression did not correlate with its copy number and it is possible that the level of expression was dependent on either its integration site or modifications such as acetylation and methylation. Thus, our NS1-transgenic mice include early foetal loss prior to liver haematopoiesis. In humans, similar early foetal loss associated with B19 infection has also been reported (Miller *et al.*, 1998). Furthermore, we showed that F1 progeny derived from the same line lived to different stages and that the levels of NS1 expression were different among the littermates. We think that the differences in NS1 expression among members of the same F1 generation may be due to differences in individual mice. Further research will be necessary to clarify the mechanisms involved.

We previously detected B19-infected erythroid-lineage cells in tissues derived from foetal patients with NIHF (Yaegashi *et al.*, 1999). These cells exhibited apoptotic features similar to UT7/Epo cells infected with B19 *in vitro* (Yaegashi *et al.*, 1999), suggesting that anaemia observed in patients with NIHF results from B19-induced cytotoxicity of erythroid-lineage cells. Since NS1 is known to possess cytotoxic activity through apoptosis, the anaemia is thought to be caused by NS1 expression in erythroid-lineage cells. Our NS1-transgenic mice provide direct evidence that NS1 expression *in vivo* in erythroid-lineage cells induces anaemia.

Previously, it has been shown that B19 infects human erythroid-lineage cells *in vivo* as well as *in vitro* preferentially through its receptor, P antigen (Brown *et al.*, 1993, 1994). However, the P antigen is reportedly expressed on foetal cardiac myocytes (Rouger *et al.*, 1987). Interestingly, B19 was found to infect myocardial cells of patients with NIHF, resulting in myocarditis (Lambot *et al.*, 1999; Porter *et al.*, 1988). Hence, not only anaemia but also myocarditis is thought to be implicated in the mechanism of B19-induced human NIHF (Morey *et al.*, 1992; Naides & Weiner, 1989). Although the GATA1 promoter is known to be activated specifically in erythroid-lineage cells, we investigated whether our transgenic mice showed NS1-induced damage to the myocardium by leakiness of transgene expression. We observed that our NS1-transgenic mice showed no damage to the myocardium, which is compatible with our previous study that B19 infection was not detected in cardiac myocytes derived from patients with NIHF (Yaegashi *et al.*, 1999). These observations suggest that NS1 expression in erythroid-lineage cells is sufficient to cause an adverse murine foetal outcome like human NIHF, which may be mediated primarily by anaemia.

In the present study, we have shown hydropic change and embryonic death induced by NS1 expression in erythroid-lineage cells in mice, suggesting that the main cause of adverse

outcome by intrauterine B19 infection in human is NS1-mediated cytotoxicity of erythroid-lineage cells. Thus, our NS1-transgenic mice are expected to be a useful model for analysing the stages of the disease *in utero*.

Recently, some cases of B19-associated non-hydropic foetal loss in the late-second and third trimesters have been reported (Tolfvenstam *et al*., 2001). Similarly, we have often encountered intrauterine foetal death with pale appearance and no hydropic change when B19 infection was detected in the foetus. These observations suggest that B19 infection may induce foetal adverse outcome without hydropic changes. Hence, further study is required to clarify whether other B19 components in addition to NS1 are involved in the foetal adverse outcome in B19 infection.

We thank Drs Masayuki Yamamoto and Jun-ichi Miyazaki for providing the plasmid pIE3.9int-polyA and the CAG-CAT-Z-transgenic mice, respectively, and Dr L. C. Ndhlovu for critical reading of the manuscript. This work was supported in part by a grant for Core Research for Evolutional Science and Technology (CREST) of the Japan Science and Technology Corporation and a Grant-in-Aid for Scientific Research of the Japan Society for the Promotion of Science.

References

Anderson, M. J., Jones, S. E., Fisher-Hoch, S. P., Lewis, E., Hall, S. M., Bartlett, C. L., Cohen, B. J., Mortimer, P. P. & Pereira, M. S. (1983). Human parvovirus, the cause of erythema infectiosum (fifth disease)? *Lancet* i, 1378.

Barbany, G., Hagberg, A., Olsson-Strömberg, U., Simonsson, B., Syvänen, A. C. & Landegren, U. (2000). Manifold-assisted reverse transcription–PCR with real-time detection for measurement of the BCR-ABL fusion transcript in chronic myeloid leukemia patients. *Clinical Chemistry* **46**, 913–920.

Bièche, I., Onody, P., Laurendeau, I., Olivi, M., Vidaud, D., Lidereau, R. & Vidaud, M. (1999). Real-time reverse transcription–PCR assay for future management of ERBB2-based clinical applications. *Clinical Chemistry* **45**, 1148–1156.

Brown, K. E. & Young, N. S. (1997). Parvovirus B19 in human disease. *Annual Review of Medicine* **48**, 59–67.

Brown, T., Anand, A., Ritchie, L. D., Clewley, J. P. & Reid, T. M. (1984). Intrauterine parvovirus infection associated with hydrops fetalis. *Lancet* ii, 1033–1034.

Brown, K. E., Anderson, S. M. & Young, N. S. (1993). Erythrocyte P antigen: cellular receptor for B19 parvovirus. *Science* **262**, 114–117.

Brown, K. E., Hibbs, J. R., Gallinella, G., Anderson, S. M., Lehman, E. D., McCarthy, P. & Young, N. S. (1994). Resistance to parvovirus B19 infection due to lack of virus receptor (erythrocyte P antigen). *New England Journal of Medicine* **330**, 1192–1196.

Cossart, Y. E., Field, A. M., Cant, B. & Widdows, D. (1975). Parvovirus-like particles in human sera. *Lancet* i, 72–73.

Doerig, C., Hirt, B., Antonietti, J. P. & Beard, P. (1990). Nonstructural protein of parvoviruses B19 and minute virus of mice controls transcription. *Journal of Virology* **64**, 387–396.

Fujiwara, Y., Browne, C. P., Cunniff, K., Goff, S. C. & Orkin, S. H. (1996). Arrested development of embryonic red cell precursors in mouse embryos lacking transcription factor GATA-1. *Proceedings of the National Academy of Sciences, USA* **93**, 12355–12358.

Kelleher, J. F., Luban, N. L., Mortimer, P. P. & Kamimura, T. (1983). Human serum 'parvovirus': a specific cause of aplastic crisis in children with hereditary spherocytosis. *Journal of Pediatrics* **102**, 720–722.

Lakso, M., Sauer, B., Mosinger, B., Jr, Lee, E. J., Manning, R. W., Yu, S.-H., Mulder, K. L. & Westphal, H. (1992). Targeted oncogene activation by site-specific recombination in transgenic mice. *Proceedings of the National Academy of Sciences, USA* **89**, 6232–6236.

Lambot, M.-A., Noël, J.-C., Peny, M.-O., Rodesch, F. & Haot, J. (1999). Fetal parvovirus B19 infection associated with myocardial necrosis. *Prenatal Diagnosis* **19**, 389.

Levy, R., Weissman, A., Blomberg, G. & Hagay, Z. J. (1997). Infection by parvovirus B19 during pregnancy: a review. *Obstetrical and Gynecological Survey* **52**, 254–259.

Miller, E., Fairley, C. K., Cohen, B. J. & Seng, C. (1998). Immediate and long term outcome of human parvovirus B19 infection in pregnancy. *British Journal of Obstetrics and Gynaecology* **105**, 174–178.

Moffatt, S., Tanaka, N., Tada, K., Nose, M., Nakamura, M., Muraoka, O., Hirano, T. & Sugamura, K. (1996). A cytotoxic nonstructural protein, NS1, of human parvovirus B19 induces activation of interleukin-6 gene expression. *Journal of Virology* **70**, 8485–8491.

Moffatt, S., Yaegashi, N., Tada, K., Tanaka, N. & Sugamura, K. (1998). Human parvovirus B19 nonstructural (NS1) protein induces apoptosis in erythroid lineage cells. *Journal of Virology* **72**, 3018–3028.

Momoeda, M., Wong, S., Kawase, M., Young, N. S. & Kajigaya, S. (1994). A putative nucleoside triphosphate-binding domain in the nonstructural protein of B19 parvovirus is required for cytotoxicity. *Journal of Virology* **68**, 8443–8446.

Morey, A. L., Keeling, J. W., Porter, H. J. & Fleming, K. A. (1992). Clinical and histopathological features of parvovirus B19 infection in human fetus. *British Journal of Obstetrics and Gynaecology* **99**, 566–574.

Morey, A. L., Ferguson, D. J. & Fleming, K. A. (1993). Ultrastructural features of fetal erythroid precursors infected with parvovirus B19 in vitro: evidence of cell death by apoptosis. *Journal of Pathology* **169**, 213–220.

Morita, E., Tada, K., Chisaka, H., Asao, H., Sato, H., Yaegashi, N. & Sugamura, K. (2001). Human parvovirus B19 induces cell cycle arrest at G_2 phase with accumulation of mitotic cyclins. *Journal of Virology* **75**, 7555–7563.

Mucenski, M. L., McLain, K., Kier, A. B., Swerdlow, S. H., Schreiner, C. M., Miller, T. A., Pietryga, D. W., Scott, W. J., Jr & Potter, S. S. (1991). A functional c-myb gene is required for normal murine fetal hepatic hematopoiesis. *Cell* **65**, 677–689.

Naides, S. J. & Weiner, C. P. (1989). Antenatal diagnosis and palliative treatment of non-immune hydrops fetalis secondary to fetal parvovirus B19 infection. *Prenatal Diagnosis* **9**, 105–114.

Onodera, K., Takahashi, S., Nishimura, S., Ohta, J., Motohashi, H., Yomogida, K., Hayashi, N., Engel, J. D. & Yamamoto, M. (1997). GATA-1 transcription is controlled by distinct regulatory mechanisms during primitive and definitive erythropoiesis. *Proceedings of the National Academy of Sciences, USA* **94**, 4487–4492.

Orban, P. C., Chui, D. & Marth, J. D. (1992). Tissue- and site-specific DNA recombination in transgenic mice. *Proceedings of the National Academy of Sciences, USA* **89**, 6861–6865.

Ozawa, K., Kurtzman, G. & Young, N. S. (1986). Replication of the B19 parvovirus in human bone marrow cell cultures. *Science* **233**, 883–886.

Ozawa, K., Ayub, J., Hao, Y.-S., Kurtzman, G., Shimada, T. & Young, N. S. (1987). Novel transcription map for the B19 (human) pathogenic parvovirus. *Journal of Virology* **61**, 2395–2406.

Ozawa, K., Ayub, J., Kajigaya, S., Shimada, T. & Young, N. S. (1988).

The gene encoding the nonstructural protein of B19 (human) parvovirus may be lethal in transfected cells. *Journal of Virology* **62**, 2884–2889.

Pevny, L., Simon, M. C., Robertson, E., Klein, W. H., Tsai, S. F., D'Agati, V., Orkin, S. H. & Constantini, F. (1991). Erythroid differentiation in chimaeric mice blocked by a targeted mutation in the gene for transcription factor GATA-1. *Nature* **349**, 257–260.

Porter, H. J., Quantrill, A. M. & Fleming, K. A. (1988). B19 parvovirus infection of myocardial cells. *Lancet* i, 535–536.

Rouger, P., Gane, P. & Salmon, C. (1987). Tissue distribution of H, Lewis and P antigens as shown by a panel of 18 monoclonal antibodies. *Revue Française de Transfusion et d'Immunohematologie* **30**, 699–708.

Sakai, K. & Miyazaki, J. (1997). A transgenic mouse line that retains Cre recombinase activity in mature oocytes irrespective of the cre transgene transmission. *Biochemical and Biophysical Research Communications* **237**, 318–324.

Shimomura, S., Komatsu, N., Frickhofen, N., Anderson, S., Kajigaya, S. & Young, N. S. (1992). First continuous propagation of B19 parvovirus in a cell line. *Blood* **79**, 18–24.

Shivdasani, R. A. & Orkin, S. H. (1996). The transcriptional control of hematopoiesis. *Blood* **87**, 4025–4039.

Socolovsky, M., Fallon, A. E. J., Wang, S., Brugnara, C. & Lodish, H. F. (1999). Fetal anemia and apoptosis of red cell progenitors in Stat5a$^{-/-}$5b$^{-/-}$ mice: a direct role for Stat5 in Bcl-X_L induction. *Cell* **98**, 181–191.

Sol, N., Morinet, F., Alizon, M. & Hazan, U. (1993). Trans-activation of the long terminal repeat of human immunodeficiency virus type 1 by the parvovirus B19 NS1 gene product. *Journal of General Virology* **74**, 2011–2014.

Sol, N., Le Junter, J., Vassias, I., Freyssinier, J. M., Thomas, A., Prigent, A. F., Rudkin, B. B., Fichelson, S. & Morinet, F. (1999). Possible interactions between the NS-1 protein and tumor necrosis factor alpha pathways in erythroid cell apoptosis induced by human parvovirus B19. *Journal of Virology* **73**, 8762–8770.

Tolfvenstam, T., Papadogiannakis, N., Norbeck, O., Petersson, K. & Broliden, K. (2001). Frequency of human parvovirus B19 infection in intrauterine fetal death. *Lancet* **357**, 1494–1497.

Yaegashi, N., Shiraishi, H., Takeshita, T., Nakamura, M., Yajima, A. & Sugamura, K. (1989). Propagation of human parvovirus B19 in primary culture of erythroid lineage cells derived from fetal liver. *Journal of Virology* **63**, 2422–2426.

Yaegashi, N., Okamura, K., Yajima, A., Murai, C. & Sugamura, K. (1994). The frequency of human parvovirus B19 infection in nonimmune hydrops fetalis. *Journal of Perinatal Medicine* **22**, 159–163.

Yaegashi, N., Niinuma, T., Chisaka, H., Watanabe, T., Uehara, S., Okamura, K., Moffatt, S., Sugamura, K. & Yajima, A. (1998). The incidence of, and factors leading to, parvovirus B19-related hydrops fetalis following maternal infection; report of 10 cases and meta-analysis. *Journal of Infection* **37**, 28–35.

Yaegashi, N., Niinuma, T., Chisaka, H., Uehara, S., Moffatt, S., Tada, K., Iwabuchi, M., Matsunaga, Y., Nakayama, M., Yutani, C., Osamura, Y., Hirayama, E., Okamura, K., Sugamura, K. & Yajima, A. (1999). Parvovirus B19 infection induces apoptosis of erythroid cells in vitro and in vivo. *Journal of Infection* **39**, 68–76.

Young, N. (1988). Hematologic and hematopoietic consequences of B19 parvovirus infection. *Seminars in Hematology* **25**, 159–172.

Received 26 July 2001; Accepted 25 October 2001